e-ISSN 2320 –7876 www.ijfans.org
Vol.11, Iss.9, Dec 2022

Research Paper

Effect of temperature on structural and magnetic properties of iron oxide nanoparticles

R. Kalpana[1,*], G. Padma Priya[1]

[1] Department of Chemistry, Faculty of Arts and Science,
Bharath Institute of Higher Education and Research (BIHER),
Chennai – 600073, Tamil Nadu, India

***Corresponding Author Email: rvkalpusrii@gmail.com** (R. Kalpana)

Address for Correspondence

R. Kalpana[1,*], G. Padma Priya[1]

[1] Department of Chemistry, Faculty of Arts and Science,
Bharath Institute of Higher Education and Research (BIHER),
Chennai – 600073, Tamil Nadu, India

***Corresponding Author Email: rvkalpusrii@gmail.com** (R. Kalpana)

Abstract

Magnetic iron oxide nanoparticles were successfully prepared by one-pot low temperature method and it was widely investigated. The phase purity and the crystal structure of the as-prepared samples were characterized by XRD and further determined by Rietveld analysis. The crystallite size was calculated using Debye Sherrer formula, and it shows the range of 15-20 nm. The lattice parameters of the samples were measured by Rietveld analysis. The morphology of the products was studied by HR-SEM and it was confirmed by HR-TEM. The observation showed that the morphology of the nanostructures changed from nanospheres into nanorods as the temperature was varied, while their size was also increased. The formation of pure α-Fe_2O_3 samples was further confirmed by EDX analysis. The optical properties and the band gap energy were measured by UV-Visible DRS and PL spectra. Magnetic hysteresis (M-H) loops revealed that the as-prepared iron oxide nanoparticles displayed ferromagnetic behavior.

Keywords: Powder X-ray diffraction; Microscopy; EDX analysis; Magnetic properties.

e-ISSN 2320 –7876 www.ijfans.org
Vol.11, Iss.9, Dec 2022

Research Paper

1. Introduction

Nano-structured magnetic iron oxide nanoparticles have attracted great attention, because of their interesting magnetic properties than those of bulk materials. Magnetic iron oxide nanoparticles are well-known and chemically reactive materials, during the past decades [1-10]. Magnetic iron oxide nanoparticles have been successfully prepared by various methods and were used in various fields [11-20]. Among these nanostructures nanotubes, nanowires and nanorods have more specific area and also exhibit excellent properties than others. To the best of our knowledge, there are only very few literatures available on the low temperature one-pot template free synthesis of magnetic iron oxide nanoparticles. Various methods have been used to develop the different morphology of Magnetic iron oxide nanoparticles including the hydrothermal, solvothermal, thermal oxidation and solution-combustion method [21-30].

One-pot low temperature synthesis is a well-known method for the preparation of magnetic iron oxide nanoparticles, and offers effective control over the size and shape of the nanostructures, than the other methods. One-pot synthesis offers several advantages, such as, high purity products, short reaction times, relatively lower temperatures, along with high homogeneity and well-crystallized products. However, the property of the samples depends on size, shape and morphology of the materials. Hence, when the size of magnetic iron oxide nanoparticles reduces to the nanometer range, it shows unusual magnetic behaviors that evidently differ from their bulk materials, due to quantum confinement effect [31-36].

2. Experimental

2.1. Materials and methods

All the chemicals used in this study were of analytical grade obtained from Merck, India and were used as received without further purification. The typical synthesis procedure for magnetic iron oxide nanoparticles is as follows: Ferric nitrate ($Fe(NO_3)_3 \cdot 9H_2O$, 98%) and ferrous sulphate ($FeSO_4.7H_2O$) were used as the precursors for this preparation. $Fe(NO_3)_3 \cdot 9H_2O$ and $FeSO_4.7H_2O$ was dissolved separately in double-distilled water to obtain clear solution. The $FeSO_4.7H_2O$ solution was slowly added into the $Fe(NO_3)_3 \cdot 9H_2O$ solution with constant stirring at room temperature. The pH of the solution was adjusted by adding ammonia (NH_3) solution and the pH is maintained at 10, and then the solution continuously stirred for 30 min at 80 ºC. A

black precipitate was obtained. The precipitate was filtered, repeatedly rinsed with distilled water, and then washed well with ethanol. The resultant solid product was dried at 80 °C for 1 h and calcined at 600 °C for 2 h.

2.2. Characterization

The structural characterization of α-Fe_2O_3 nanostructures were performed using Rigaku Ultima X-ray diffractometer equipped with Cu-Kα radiation (λ=1.5418 Å). Structural refinements using the Rietveld method was carried out by PDXL program; both refined lattice parameter and crystallite size of the obtained samples were reported. Morphological studies and EDX of magnetic iron oxide nanoparticles have been performed with a Jeol JSM6360 HR-SEM. The transmission electron micrographs were carried out by Philips-TEM (CM20) to confirm the morphology and crystallite size of the samples. The surface area of the samples was derived from the nitrogen adsorption-desorption isotherms using liquid nitrogen at 77 K using an automatic adsorption instrument (Quantachrome Corp. Nova-1000 gas sorption analyzer). The UV-Visible DRS spectrum was recorded using Cary100 UV-Visible spectrophotometer to estimate their band gap energy. The PL properties were recorded at room temperature using Varian Cary Eclipse Fluorescence Spectrophotometer. Magnetic measurements were carried out at room temperature using a PMC MicroMag 3900 model VSM equipped with 1 Tesla magnet.

3. Results and discussion

3.1 Structural analysis

The crystal structure and phase purity of the as-prepared α-Fe_2O_3 samples were confirmed by analyzing the XRD analysis. Fig.1 shows the XRD patterns of magnetic iron oxide nanoparticles. The observed diffraction peaks are associated with [012], [110], [024], [116], [018], [300], and [220] plane respectively, which can be readily assigned to rhombohedral phase of magnetic iron oxide nanoparticles [24]. The XRD patterns did not show any traces of other phases of iron oxide nanoparticles, thus confirming the high purity of iron oxide nanoparticles. The average crystallite size of the samples was calculated using the Debye Scherrer formula [25] is given in Eq. (1):

$$L = \frac{0.89\lambda}{\beta \cos\theta} \qquad \text{--- (1)}$$

e-ISSN 2320 –7876 www.ijfans.org
Research Paper
Vol.11, Iss.9, Dec 2022

where L is the average particle, λ, the X-ray wavelength (0.1542 nm), β, full width at half maximum (FWHM) and θ, the Bragg angle. The crystallite size (L) of iron oxide nanoparticles is 19 nm, due to the high temperature calcination (600 ºC) [26].

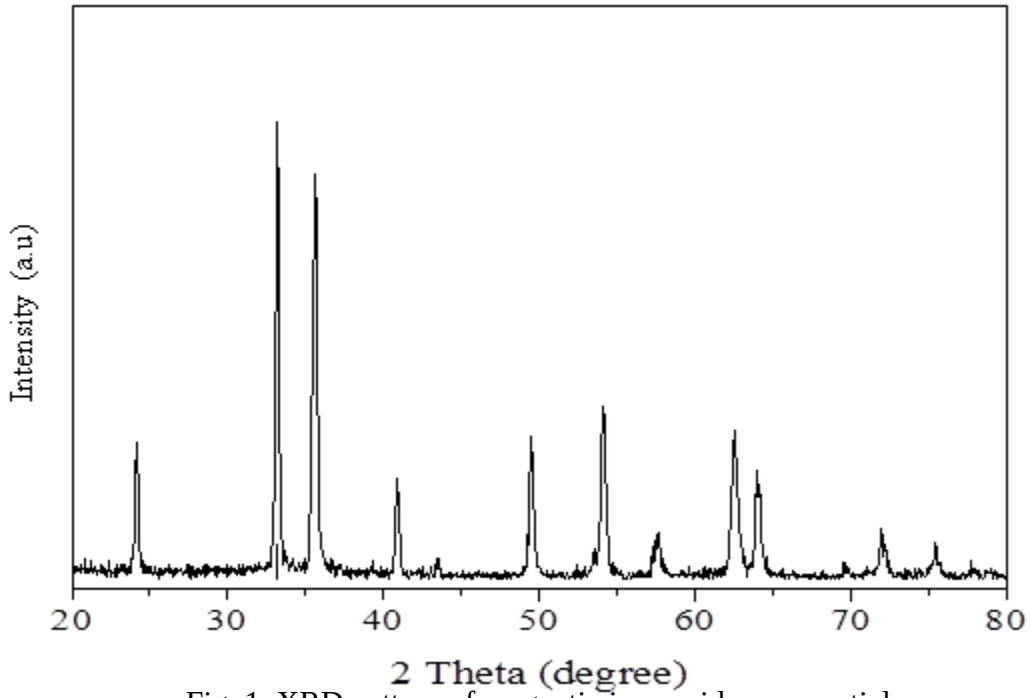

Fig. 1. XRD pattern of magnetic iron oxide nanoparticles.

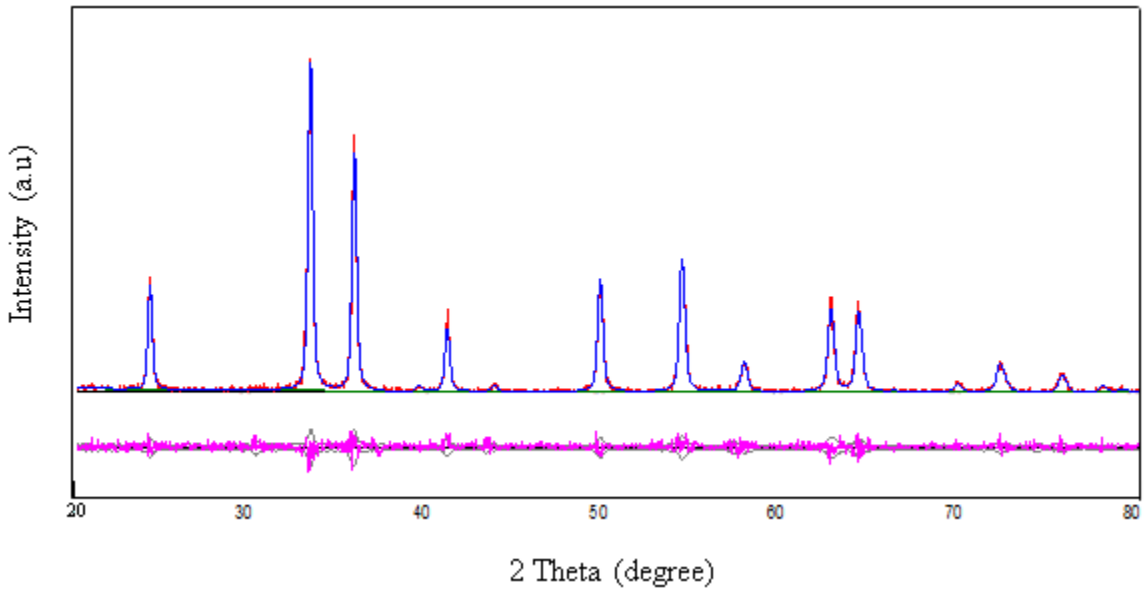

Fig. 2. Rietveld XRD pattern of magnetic iron oxide nanoparticles.

e-ISSN 2320 –7876 www.ijfans.org
Research Paper
Vol.11, Iss.9, Dec 2022

Fig. 2 shows the Rietveld refinement XRD analysis of iron oxide nanoparticles. The crystallite size increases with an increase in the calcinations temperature. This observation may be attributed to the particles growth and aggregation of small particles after being calcined at higher temperatures (600 ºC/2 h) [27].

3.2. Scanning electron microscopy (SEM) studies

The morphological characteristics of the obtained magnetic iron oxide nanoparticles were investigated by HR-SEM studies. Fig. 3 shows the HR-SEM images of magnetic iron oxide nanoparticles with agglomeration. The particle size of magnetic iron oxide nanoparticles is around 15-20 nm, because it is exposed to heat for more time, which results in the formation of bigger particles, (i.e) it may be due to the sintering effect in magnetic iron oxide nanoparticles.

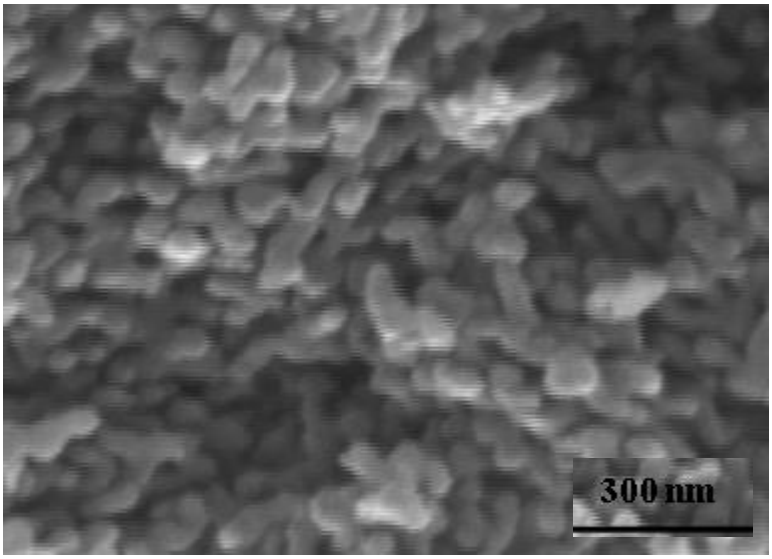

Fig. 3. HR-SEM images of magnetic iron oxide nanoparticles.

3.3. Transmission electron microscopy (TEM) studies

Fig. 4 shows the HR-TEM images of magnetic iron oxide nanoparticles. The average particle size and void space diameter of magnetic iron oxide nanoparticles were found to be 15-20 nm for magnetic iron oxide nanoparticles. A selected-area electron diffraction pattern (SAED) of the magnetic iron oxide nanoparticles are shown in the inset of Fig. 4, which correlated well with the XRD and Rietveld results. The SAED pattern implies that the as-prepared magnetic iron

oxide nanoparticles are good single crystalline materials. There is no evidence for more than one pattern, suggesting the single phase nature of the material.

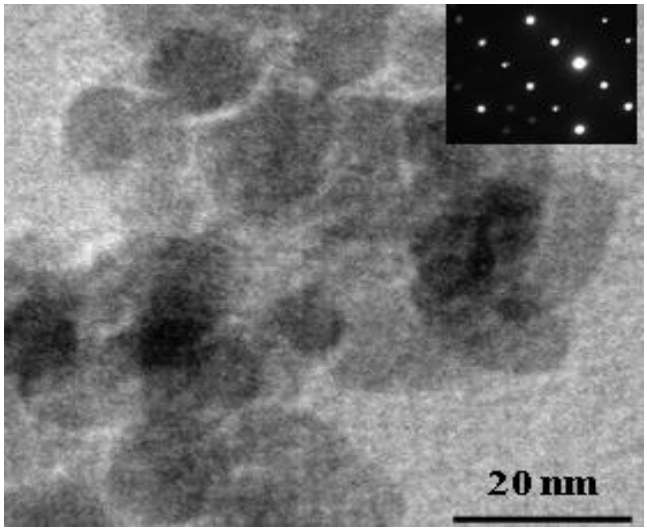

Fig. 4. HR-TEM images of magnetic iron oxide nanoparticles.

3.4. Energy dispersive X-ray (EDX) analysis

Fig. 5 shows the EDX analysis of the as-prepared magnetic iron oxide nanoparticles. It reveals the presence of O and Fe elements and no signals of other elements present indicating that the as-synthesized products are pure. A small peak is appeared at 2.1 KeV for both samples, which indicates the presence of gold (Au) peak that has been used as a sputter coating, while preparing the sample for HR-SEM analysis for the better visibility of the surface morphology.

e-ISSN 2320 –7876 www.ijfans.org
Research Paper
Vol.11, Iss.9, Dec 2022

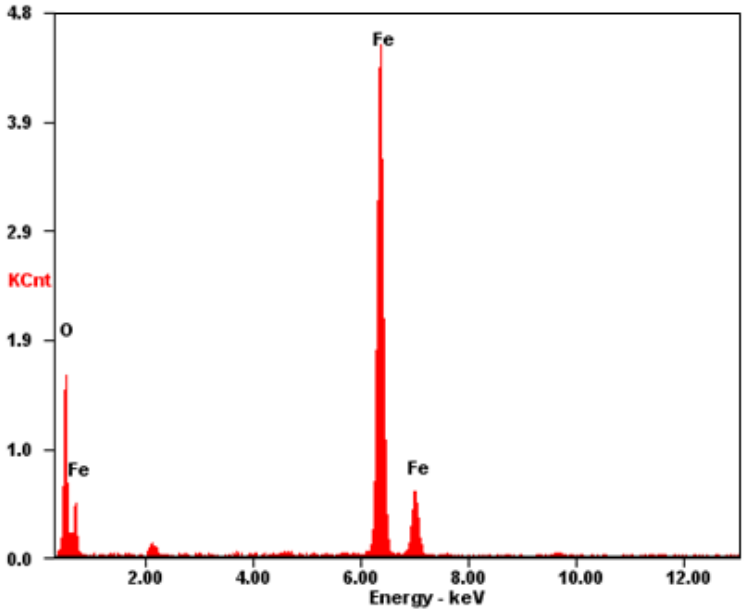

Fig. 5. EDX spectrs of magnetic iron oxide nanoparticles.

3.5. Diffuse reflectance spectroscopy (DRS)

The optical properties of the as-prepared magnetic iron oxide nanoparticles were studied by the UV-Vis DRS techniques. The energy band gap (E_g) of magnetic iron oxide nanoparticles can be evaluated from the E_g measurements using Kubelka-Munk (K-M) model and the F(R) is estimated using the formula [31] given in Eq. (3)

$$F(R) = (1-R)^2 / 2R \quad \text{---- (3)}$$

where F(R), is the Kubelka-Munk function, R, is the reflectance. A graph is plotted between $[F(R)h\upsilon]^2$ and $h\upsilon$, the intercept value is the band gap energy as shown in Fig. 6. The decrease in band gap energy is due to the size effect, i.e. the crystallite size is increased with increasing the temperature.

e-ISSN 2320 –7876 www.ijfans.org
Research Paper
Vol.11, Iss.9, Dec 2022

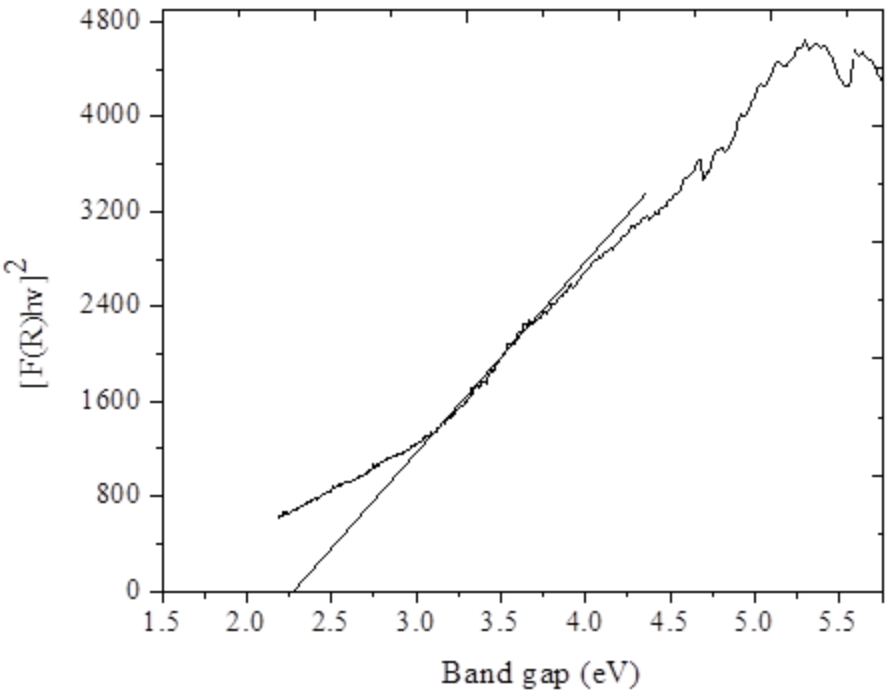

Fig. 6. UV-Vis DRS spectra of magnetic iron oxide nanoparticles.

3.5 Photoluminescence (PL) studies

The PL spectrum of magnetic iron oxide nanoparticles was measured at room temperature as shown in Fig. 7. The PL spectra can be used to study the quantum size effect and structural defects. A strong peak appeared at around at 450 nm for magnetic iron oxide nanoparticles, can be attributed to the band-band PL phenomenon [40], may be attributed to the oxygen vacancies giving rise to green emissions. The intensity of these peaks increases with increase the calcinations temperature, which produce good crystallinity of magnetic iron oxide nanoparticles. The band gap emissions mainly indicate the various structural defects such as oxygen vacancies. The oxygen vacancies are familiar to be great electron scavengers, which is better for photo-activity [41].

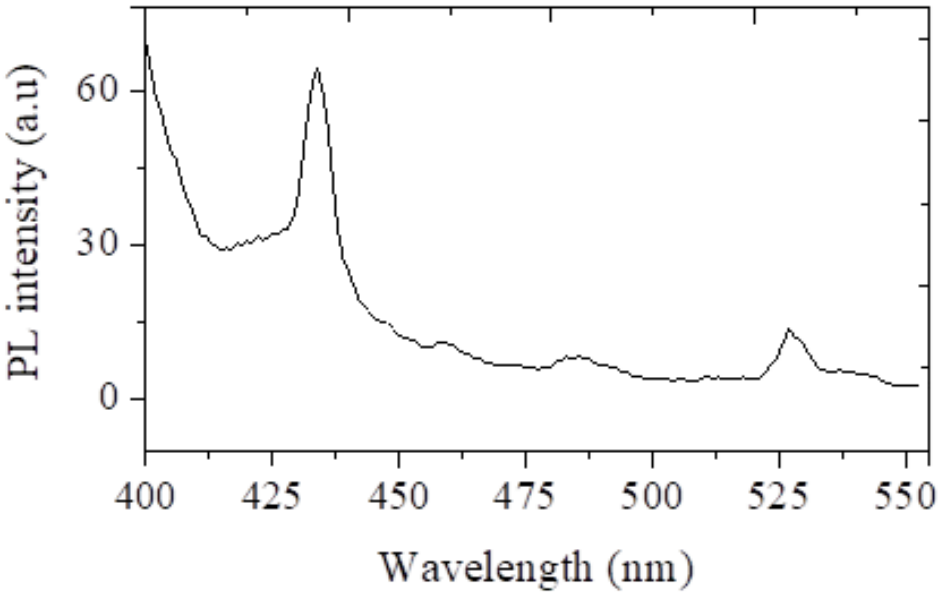

Fig. 7. PL spectra of magnetic iron oxide nanoparticles.

3.7. VSM measurements

Magnetic properties of magnetic iron oxide nanoparticles were carried out using room temperature VSM with the applied filed range of -10 to +10 kOe. Magnetic iron oxide nanoparticles are an important magnetic material and shows unusual magnetic behavior, due to their particle size and morphology of the samples [42]. Fig. 8 shows the magnetic hysteresis (M-H) loops of magnetic iron oxide nanoparticles. The observed results indicated a ferromagnetic behavior. VSM measurements were carried out to investigate the influence of temperature and morphologies on their magnetic properties.

e-ISSN 2320 –7876 www.ijfans.org
Vol.11, Iss.9, Dec 2022

Research Paper

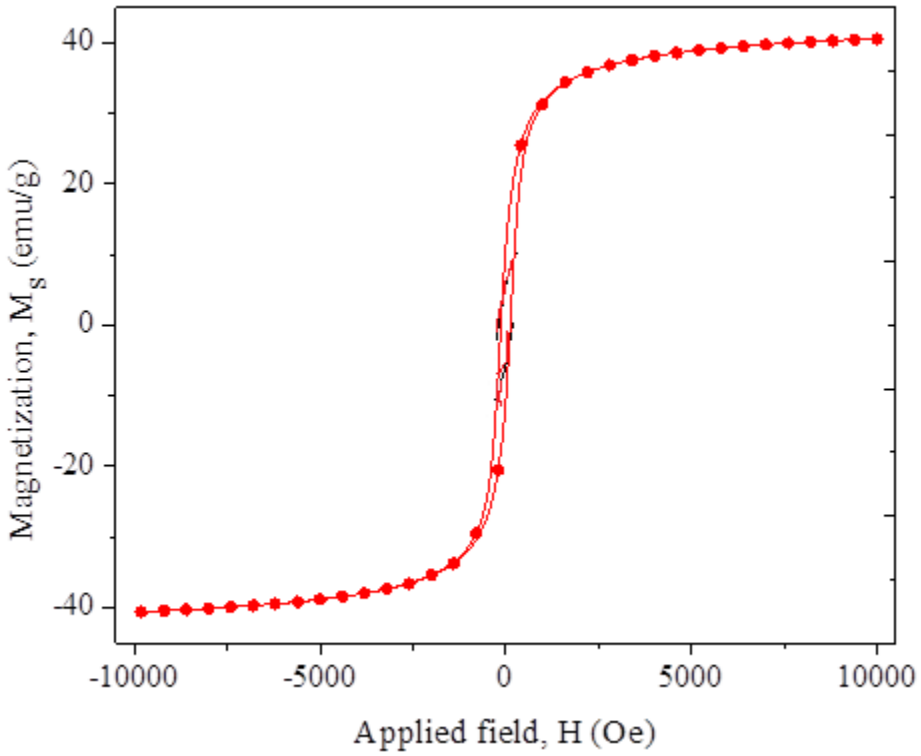

Fig. 8. VSM spectra of magnetic iron oxide nanoparticles.

4. Conclusions

Magnetic iron oxide nanoparticles were successfully prepared by one-pot low temperature synthesis. The morphology of the magnetic iron oxide nanoparticles depends on calcination temperature,. The crystallite size was also increased, when the temperature is varied. The formation of single and pure phase was confirmed by XRD and EDX analysis. Magnetic measurements revealed that magnetic iron oxide nanoparticles show ferromagnetic behaviorHence this method is an economical and rapid method for the preparation of magnetic iron oxide nanoparticles, in the better optical and magnetic properties.

References

[1]. S. S. Al-Jameel, M. A. Almessiere, F. A. Khan, N. Taskhandi , Y. Slimani, N. S. Al-Saleh, A. Manikandan, E. A. Al-Suhaimi, A. Baykal, Synthesis, Characterization, Anti-Cancer Analysis of $Sr_{0.5}Ba_{0.5}Dy_xSm_xFe_{8-2x}O_{19}$ ($0.00 \leq x \leq 1.0$) Microsphere Nanocomposites, Nanomaterials, 11 (2021) 700.

[2]. M. A. Almessiere, Y. Slimani, H. Güngüneş, K. A. Demir, Z. Tatiana, T. Sergei, T. Alex, A. Manikandan, A. Fatimah, A. Baykal, Influence of Dy^{3+} ions on microstructure, magnetic, electrical and microwave properties of $[Ni_{0.4}Cu_{0.2}Zn_{0.4}](Fe_{2-x}Dy_x)O_4$ ($0.00<x<0.04$) spinel ferrites, ACS Omega, 6 (2021) 10266-10280.

[3]. P. Annie Vinosha, A. Manikandan, A. Christy Preetha, A. Dinesh, Y. Slimani, M.A. Almessiere, A. Baykal, Belina Xavier, G. Francisco Nirmala, Review on recent advances of synthesis, magnetic properties and water treatment applications of cobalt ferrite nanoparticles and nanocomposites, Journal of Superconductivity and Novel Magnetism, 34 (2021) 995–1018.

[4]. K. Elayakumar, A. Manikandan, A. Dinesh, K. Thanrasu, K. Kanmani Raja, R. Thilak Kumar, Y. Slimani, S. K. Jaganathan, A. Baykal, Enhanced magnetic property and antibacterial biomedical activity of Ce^{3+} doped $CuFe_2O_4$ spinel nanoparticles synthesized by sol-gel method, J. Magn. Magn. Mater. 478 (2019) 140–147.

[5]. A. Godlyn Abraham, A. Manikandan, E. Manikandan, S. Vadivel, S. K. Jaganathan, A. Baykal, P. Sri Renganathan, Enhanced magneto-optical and photo-catalytic properties of transition metal cobalt (Co^{2+} ions) doped spinel $MgFe_2O_4$ ferrite nanocomposites, J. Magn. Magn. Mater. 452 (2018) 380-388.

[6]. M. Maria Lumina Sonia, S. Anand, S. Blessi, S. Pauline, A. Manikandan, Effect of surfactants (PVB/EDTA/CTAB) assisted sol-gel synthesis on structural, magnetic and dielectric properties of $NiFe_2O_4$ nanoparticles, Ceram. Int. 44 (2018) 22068-22079.

[7]. K. Elayakumar, A. Dinesh, A. Manikandan, P. Murugesan, G. Kavitha, S. Prakash, R. Thilak Kumar, S. K. Jaganathan, A. Baykal, Structural, morphological, enhanced magnetic properties and antibacterial bio-medical activity of rare earth element (REE) Cerium (Ce^{3+}) doped $CoFe_2O_4$ nanoparticles, J. Magn. Magn. Mater. 476 (2019) 157-165.

[8]. Md Amir, H. Gungunes, A. Baykal, M. Almessiere, H. Sozeri, I. Ercan, M. Sertkol, S. Asiri, A Manikandan, Effect of annealing temperature on Magnetic and Mossbauer properties of $ZnFe_2O_4$ nanoparticles by sol-gel approach, J. Supercond. Nov. Magn. 31 (2018) 3347–3356.

[9]. I. J. C. Lynda, M. Durka, A. Dinesh, A. Manikandan, S. K. Jaganathan, A. Baykal, S. Arul Antony, Enhanced Magneto-optical and Photocatalytic Properties of Ferromagnetic $Mg_{1-y}Ni_yFe_2O_4$ ($0.0 \leq y \leq 1.0$) Spinel Nano-ferrites, J. Supercond. Nov. Magn. 31 (2018) 3637–3647.

[10]. M. Maria Lumina Sonia, S. Anand, V. Maria Vinosel, M. Asisi Janifer, S. Pauline, A. Manikandan, Effect of lattice strain on structure, morphology and magneto-dielectric properties of $NiGd_xFe_{2-x}O_4$ ferrite nano-crystallites synthesized by sol-gel route, J. Magn. Magn. Mater. 466 (2018) 238-251.

[11]. A. Godlyn Abraham, A. Manikandan, E. Manikandan, S. K. Jaganathan, A. Baykal, P. Sri Renganathan, Enhanced Opto-Magneto Properties of $Ni_xMg_{1-x}Fe_2O_4$ ($0.0 \leq x \leq 1.0$) Ferrites Nano-Catalysts, J. Nanoelect. Optoelect. 12 (2017) 1326–1333

[12]. S. Asiri, M. Sertkol, S. Guner, H. Gungunes, K.M. Batoo, T.A. Saleh, H. Sozeri, M.A. Almessiere, A. Manikandan, A. Baykal, Hydrothermal synthesis of $Co_yZn_yMn_{1-2y}Fe_2O_4$ nanoferrites: Magneto-optical investigation, Ceram. Int. 44 (2018) 5751–5759.

[13]. A. Baykal, S. Guner, H. Gungunes, K.M. Batoo, Md. Amir, A. Manikandan, Magneto Optical Properties and hyperfine interactions of Cr^{3+} ion substituted copper ferrite nanoparticles, J. Inorg. Organomet. Polym. 28 (2018) 2533–2544,

[14]. E. Hema, A. Manikandan, P. Karthika, M. Durka, S. Arul Antony, B. R. Venkatraman, Magneto-optical properties of recyclable spinel $Ni_xMg_{1-x}Fe_2O_4$ ($0.0 \leq x \leq 1.0$) nano-catalysts, J. Nanosci. Nanotech. 16 (2016) 7325-7336.

[15]. Y. Slimani, A. Baykal, Md. Amir, N. Tashkandi, H. Güngüneş, S. Guner, H.S. El Sayed, F. Aldakheel, T.A. Saleh, A. Manikandan, Substitution effect of Cr^{3+} on hyperfine interactions, magnetic and optical properties of Sr-hexaferrites, Ceram. Int. 44 (2018) 15995-16004.

[16]. Y. Slimani, H. Gungunes, M. Nawaz, A. Manikandan, H.S. El Sayed, M.A. Almessiere, H. Sozeri, S.E. Shirsath, I. Ercan, A. Baykal, Magneto-optical and microstructural properties of spinel cubic copper ferrites with Li-Al co-substitution, Ceram. Int. 44 (2018) 14242-14250.

[17]. S. Asiri, S. Güner, A. Demir, A. Yildiz, A. Manikandan, A. Baykal, Synthesis and Magnetic Characterization of Cu Substituted Barium Hexaferrites, J. Inorg. Organomet. Polym. Mater. 28 (2018) 1065–1071.

[18]. A. Silambarasu, A. Manikandan, K. Balakrishnan, Room temperature superparamagnetism and enhanced photocatalytic activity of magnetically reusable spinel $ZnFe_2O_4$ nano-catalysts, J. Supercond. Nov. Magn. 30 (2017) 2631–2640.

[19]. G. Padmapriya, A. Manikandan, V. Krishnasamy, S. K. Jaganathan, S. Arul Antony, Enhanced catalytic activity and magnetic properties of spinel $Mn_xZn_{1-x}Fe_2O_4$ ($0.0 \leq x \leq 1.0$) nano-photocatalysts by microwave irradiation route, J. Supercond. Nov. Magn. 29 (2016) 2141-2149.

[20]. S. Gunasekaran, K. Thanrasu, A. Manikandan, M. Durka, A. Dinesh, S. Anand, S. Shankar, Y.Slimani, M. A. Almessiere, A. Baykal, Structural, fabrication and enhanced electromagnetic wave absorption properties of reduced graphene oxide (rGO)/zirconium substituted cobalt ferrite ($Co_{0\cdot5}Zr_{0\cdot5}Fe_2O_4$) nanocomposites, Physica B: Condensed Matter, 605 (2021) 412784.

[21]. F. Hussain, S. Z. Shah, H. Ahmad, S. A. Abubshait, H. A. Abubshait, A. Laref, A. Manikandan, H. S. Kusuma, M. Iqbal, Microalgae an ecofriendly and sustainable wastewater treatment option: Biomass application in biofuel and bio-fertilizer production. A review, Renewable and Sustainable Energy Reviews, 137 (2021) 110603.

[22]. P. A. Vinosha, A. Manikandan, A. S. J. Ceicilia, A. Dinesh, G. F. Nirmala, A. Christy Preetha, Y. Slimani, M.A. Almessiere, A. Baykal, B. Xavier, Review on recent advances of zinc substituted cobalt ferrite nanoparticles: Synthesis characterization and diverse applications, Ceramics International, 47 (2021) 10512-10535.

[23]. S. Blessi, S. Anand, A. Manikandan, M. M. Lumina Sonia, V. Maria Vinosel, Y. Slimani, M.A. Almessiere, A. Baykal, Structural, optical and electrochemical investigations of Sb

substituted mesoporous SnO_2 nanoparticles, Journal of Materials Science: Materials in Electronics, 32 (2021) 4132–4145.

[24]. Y. Slimani, N. A. Algarou, M. A. Almessiere, A. Sadaqat M. G. Vakhitov, D. S. Klygach, D. I. Tishkevich, A. V. Trukhanov, S. Güner, A. S. Hakeem, I. A. Auwal, A. Baykal, A. Manikandan, I. Ercan, Fabrication of exchanged coupled hard/soft magnetic nanocomposites: Correlation between composition, magnetic, optical and microwave properties, Arabian Journal of Chemistry, 10 (2021) 102992.

[25]. P. Manimaran, S. Balasubramaniyan, M. Azam, D. Rajadurai, S. I. Al-Resayes, G. Mathubala, A. Manikandan, S. Muthupandi, Z. Tabassum, I. Khan, Synthesis, Spectral Characterization and Biological Activities of Co(II) and Ni(II) Mixed Ligand Complexes, Molecules, 26 (2021) 823.

[26]. O. Alagha, N. Ouerfelli, H. Kochkar, M. A. Almessiere , Y. Slimani, A. Manikandan, A. Baykal, A. Mostafa, M. Zubair, M. H. Barghouthi, Kinetic Modeling for Photo-Assisted Penicillin G Degradation of $(Mn_{0.5}Zn_{0.5})[Cd_xFe_{2-x}]O_4$ ($x \leq 0.05$) Nanospinel Ferrites, Nanomaterials, 11 (2021) 970.

[27]. M. R. Ranjitha, A. Manikandan, J. N. Baby, K. Panneerselvam, S. Ragu, Mary George, Y. Slimani, M.A. Almessiere, A. Baykal, Hexagonal basalt-like ceramics $La_xMg_{1-x}TiO_3$ (x = 0 and 0.5) contrived via deep eutectic solvent for selective electrochemical detection of dopamine, Physica B: Condensed Matter, 615 (2021) 413068.

[28]. M. A. Almessiere, B. Unal, I.A. Auwal, Y. Slimani, H. Aydin, A. Manikandan, A. Baykal, Impact of calcination temperature on electrical and dielectric properties of $SrGa_{0.05}Fe_{11.98}O_4$-$Zn_{0.5}Ni_{0.5}Fe_2O_4$ hard/soft nanocomposites, Journal of Materials Science: Materials in Electronics, 32 (2021) 16589-16600.

[29]. K. Geetha, R. Udhayakumar, A. Manikandan, Enhanced magnetic and photocatalytic characteristics of cerium substituted spinel $MgFe_2O_4$ ferrite nanoparticles, Physica B: Physics of Condensed Matter, 615 (2021) 413083.

[30]. S. S. Al-Jameel, S. Rehman, M. A. Almessiere, F. A. Khan, Y. Slimani, N. S. Al-Saleh, A. Manikandan, E. A. Al-Suhaimi, A. Baykal, Anti-microbial and anti-cancer activities of

$MnZnDy_xFe_{2-x}O_4$ ($x \leq 0.1$) nanoparticles, Artificial Cells, Nanomedicine and Biotechnology, 49 (2021) 493-499.

[31]. S. Rehman, M. A. Almessiere, S. S. Al-Jameel, U. Ali, Y. Slimani, N. Taskhandi, N. S. Al-Saleh, A. Manikandan, F. A. Khan, E. A. Al-Suhaimi, A. Baykal, Designing of $Co_{0.5}Ni_{0.5}Ga_xFe_{2-x}O_4$ ($0.0 \leq x \leq 1.0$) Microspheres via Hydrothermal Approach and Their Selective Inhibition on the Growth of Cancerous and Fungal Cells, Pharmaceutics, 13 (2021) 962.

[32]. M. A. Almessiere, B. Unal, Y. Slimani, H. Gungunes, M. S. Toprak, N. Tashkand, A. Baykal, M. Sertkol, A.V. Trukhanov, A. Yıldız, A. Manikandan, Effects of Ce-Dy rare earths co-doping on various features of Ni-Co spinel ferrite microspheres prepared via hydrothermal approach, J. of Materials Research and Technology, 14 (2021) 2534-2553.

[33]. S. Blessi, A. Manikandan, S. Anand, M. M. L. Sonia, V. M. Vinosel, P. Paulraj, Y. Slimani, M.A. Almessiere, M. Iqbal, S. Guner, A. Baykal, Effect of Zinc substitution on the physical and electrochemical properties of mesoporous SnO_2 nanomaterials, Materials Chemistry and Physics, 273 (2021) 125122.

[34]. M. A. Almessiere, Y. Slimani, Y. O. Ibrahim, M. A. Gondal, M. A. Dastageer, I. A. Auwal, A. V. Trukhanov, A. Manikandan, A. Baykal, Morphological, structural, and magnetic characterizations of hard-soft ferrite nanocomposites synthesized via pulsed laser ablation in liquid, Materials Science and Engineering B, 273 (2021) 115446.

[35]. S. Blessi, S. Anand, A. Manikandan, M. Maria Lumina Sonia, V. Maria Vinosel, Y. Slimani, M.A. Almessiere, A. Baykal, Influence of Ni substitution on opto-magnetic and electrochemical properties of CTAB capped mesoporous SnO_2 nanoparticles, Journal of Materials Science: Materials in Electronics, Journal of Materials Science: Materials in Electronics, 32 (2021) 7630–7646.

[36]. M. George, T.L. Ajeesha, A. Manikandan, Ashwini Anantharaman, R.S. Jansi, E. Ranjith Kumar, Y. Slimani, M.A. Almessiere, A. Baykal, Evaluation of Cu-$MgFe_2O_4$ spinel nanoparticles for photocatalytic and antimicrobial activates, Journal of Physics and Chemistry of Solids, 153 (2021) 110010.